

Supporting Information for:

A Comparison of Non-Covalent Interactions in the Crystal Structures of two σ -Alkane Complexes of Rh Exhibiting Contrasting Stabilities in the Solid State.

M. Arif Sajjad,¹ Stuart A. Macgregor*,¹ and Andrew S. Weller²

1. Institute of Chemical Sciences, Heriot-Watt University, Edinburgh, EH14 4AS. email:
s.a.macgregor@hw.ac.uk; ORCID: 0000-0003-3454-6776

2. Department of Chemistry, University of York, Heslington, York, YO10 5DD; ORCID: 0000-0003-1646-8081

Table of Contents.

S1. Computational Details for Periodic DFT Calculations with References	pS-2
S2. CrystalExplorer Analyses	pS-3
S3. QTAIM Analyses	pS-7
S4. IGMH Plots	pS-20
S5. Correlation Plots.	pS-28

S1. Computational Details for Periodic DFT Calculations with References

Static Kohn-Sham DFT calculations were performed on periodic models of the studied rhodium complexes, employing the Gaussian Plane Wave (GPW) formalism as implemented in the QUICKSTEP¹ module within the CP2K program suite (Version 5.0).² Molecularly optimized basis sets of double- ζ quality plus polarization in their short-range variant (DZVP-MOLOPT-SR-GTH)³ were used on all atomic species. The interaction between the core electrons and the valence shell (Rh: 17, B: 3, C: 4, P: 5, F: 7, H: 1 electrons) was described by Goedecker-Teter-Hutter (GTH) pseudo potentials.⁴⁻⁶ Geometry optimisations employed the PBE GGA functional⁷ and included dispersion effects via Grimme's D3 correction.⁸ The auxiliary plane wave basis set was truncated at a cutoff of 500 Ry. The maximum force convergence criterion was set to 10^{-4} Eh·Bohr⁻¹, whilst default values were used for the remaining criteria. The convergence criterion for the self-consistent field (SCF) accuracy was set to 10^{-7} Eh and 10^{-8} Eh for geometry optimizations and vibrational analysis, respectively. The Brillouin zone was sampled using the Γ -point. Initial coordinates for [1-NBA][BAr^F₄]⁹ and [1-propane][BAr^F₄]¹⁰ were obtained from the experimental crystallographic data. Periodic boundary conditions (PBC) were applied throughout in combination with fixed unit cell parameters obtained from experiment.

Cartesian coordinates in Å of the central cations surrounded by the octahedral arrays of anions are provided as a separate XYZ file. Individual ion-pair geometries were taken from these structures without further modification.

References.

1. J. VandeVondele, M. Krack, F. Mohamed, M. Parrinello, T. Chassaing, J. Hutter, 'Quickstep: Fast and Accurate Density Functional Calculations Using a Mixed Gaussian and Plane Waves Approach' *Comput. Phys. Commun.* **2005**, *167*, 103-128.
2. J. Hutter, M. Iannuzzi, F. Schiffmann, J. VandeVondele, 'cp2k: atomistic simulations of condensed matter systems' *Wiley Interdiscip. Rev. Comput. Mol. Sci.* **2014**, *4*, 15-25.
3. T. D. Kühne, M. Iannuzzi, M. D. Ben, V. V. Rybkin, P. Seewald, F. Stein, T. Laino, R. Z. Khalilullin, O. Schütt, F. Schiffmann, D. Golze, J. Wilhelm, S. Chulkov, M. H. Bani-Hashemian, V. Weber, U. Borštník, M. Taillefumier, A. S. Jakobovits, A. Lazzaro, H. Pabst, T. Müller, R. Schade, M. Guidon, S. Andermatt, N. Holmberg, G. K. Schenter, A. Hehn, A. Bussy, F. Belleflamme, G. Tabacchi, A. Glöß, M. Lass, I. Bethune, C. J. Mundy, C. Plessl, M. Watkins, J. VandeVondele, M. Krack, J. Hutter, 'CP2K: An Electronic Structure and Molecular Dynamics Software Package - Quickstep: Efficient and Accurate Electronic Structure Calculations' *J. Chem. Phys.* **2020**, *152*, 194103.
4. S. Goedecker, M. Teter, J. Hutter, 'Separable dual-space Gaussian pseudopotentials' *Phys. Rev. B* **1996**, *54*, 1703-1710.
5. C. Hartwigsen, S. Goedecker, J. Hutter, 'Relativistic separable dual-space Gaussian pseudopotentials from H to Rn' *Phys. Rev. B* **1998**, *58*, 3641-3662.
6. M. Krack, 'Pseudopotentials for H to Kr optimized for gradient-corrected exchange-correlation functionals' *Theor. Chem. Acc.* **2005**, *114*, 145-152.7. J. P. Perdew, K. Burke, M. Ernzerhof, 'Generalized Gradient Approximation Made Simple' *Phys. Rev. Lett.* **1996**, *77*, 3865-3868.
8. S. Grimme, J. Antony, S. Ehrlich, H. Krieg, 'A Consistent and Accurate Ab Initio Parametrization of Density Functional Dispersion Correction (DFT-D) for the 94 Elements H-Pu' *J. Chem. Phys.* **2010**, *132*, 154104.
9. S. D. Pike, F. M. Chadwick, N. H. Rees, M. P. Scott, A. S. Weller, T. Krämer and S. A. Macgregor, *J. Am. Chem. Soc.*, 2015, **137**, 820-833.
10. A. J. Bukvic, A. L. Burnage, G. J. Tizzard, A. J. Martínez-Martínez, A. I. McKay, N. H. Rees, B. E. Tegner, T. Krämer, H. Fish, M. R. Warren, S. J. Coles, S. A. Macgregor and A. S. Weller, *J. Am. Chem. Soc.*, 2021, **143**, 5106-5120.

S2. CrystalExplorer Analyses

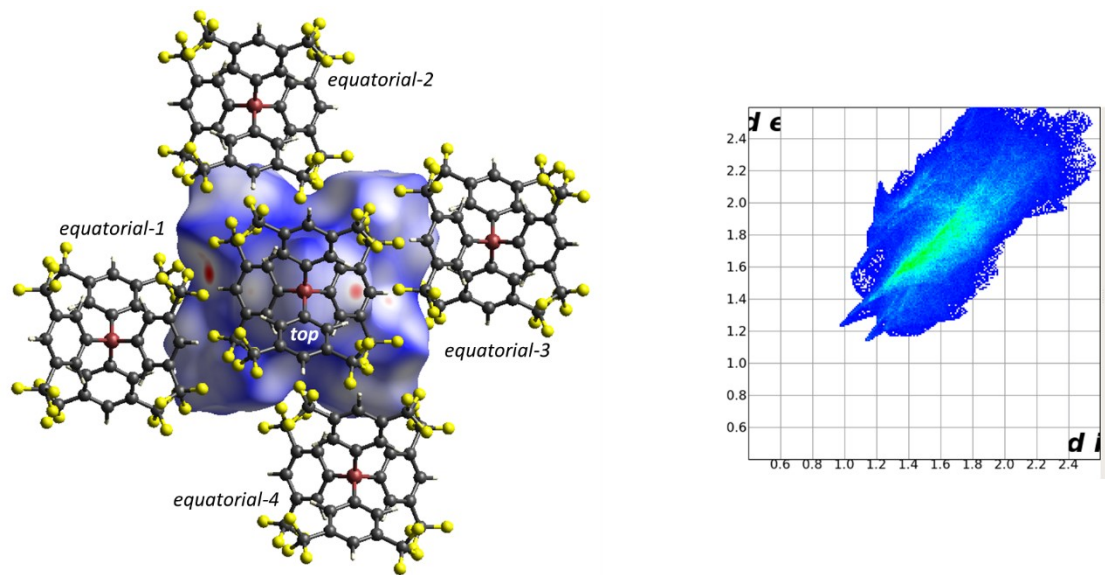


Figure S1. Hirshfeld surface mapped over d_{norm} for $[\text{1-propane}]^+$ within the octahedral array of neighbouring $[\text{BArF}_4]^-$ anions. The accompanying fingerprint plot is also displayed. The view is taken from above the ‘top’ anion looking down the $\text{B}_{\text{top}} \square \text{Rh} \square \text{B}_{\text{bottom}}$ axis.

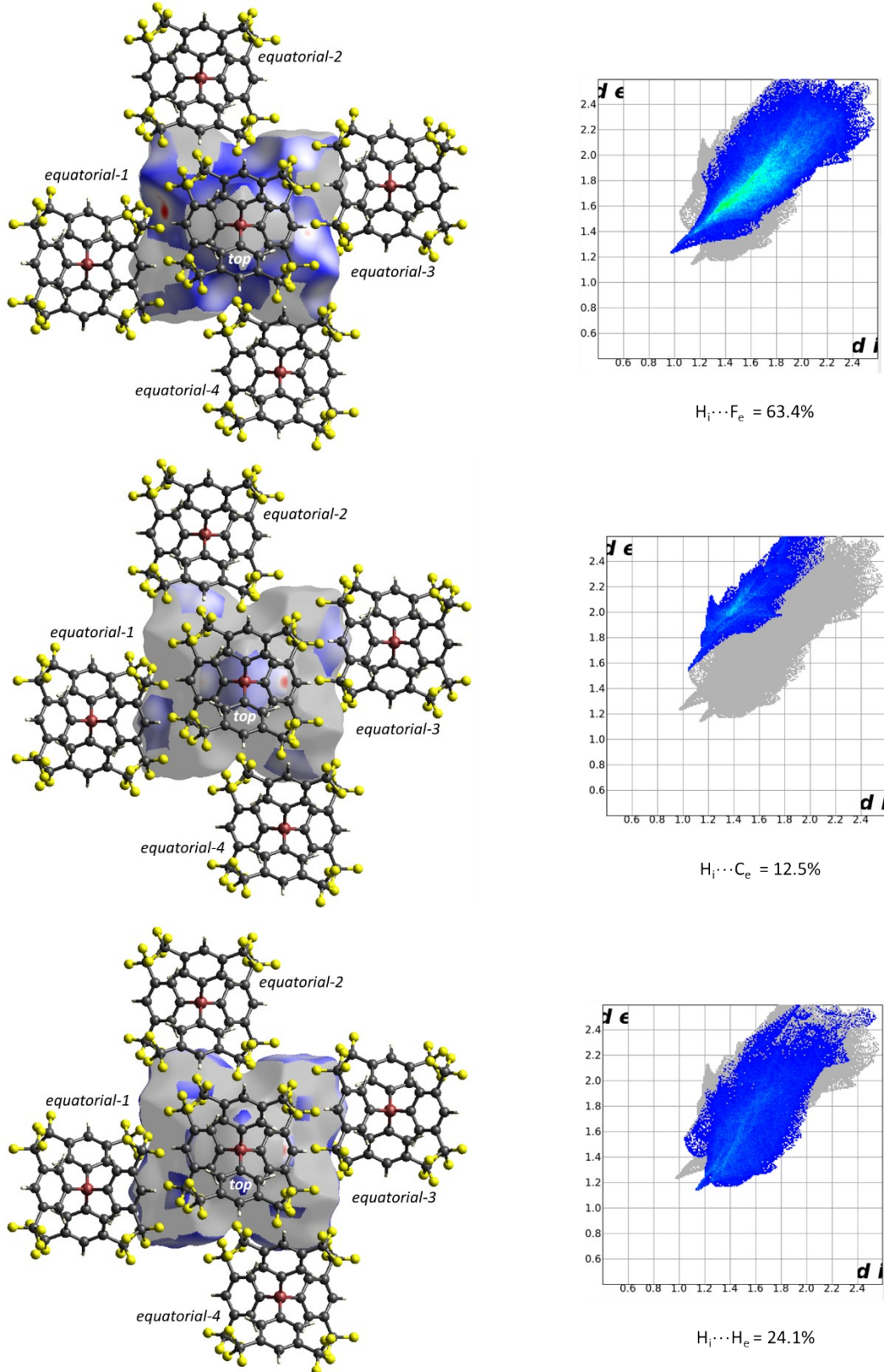


Figure S2. Hirshfeld surfaces for individual atom types mapped over d_{norm} for $[\text{1-propane}]^+$ within the octahedral array of neighbouring $[\text{BArF}_4]^-$ anions. The accompanying fingerprint plot is also displayed. The views are taken from above the 'top' anion' looking down the $\text{B}_{\text{top}} \square \text{Rh} \square \text{B}_{\text{bottom}}$ axis.

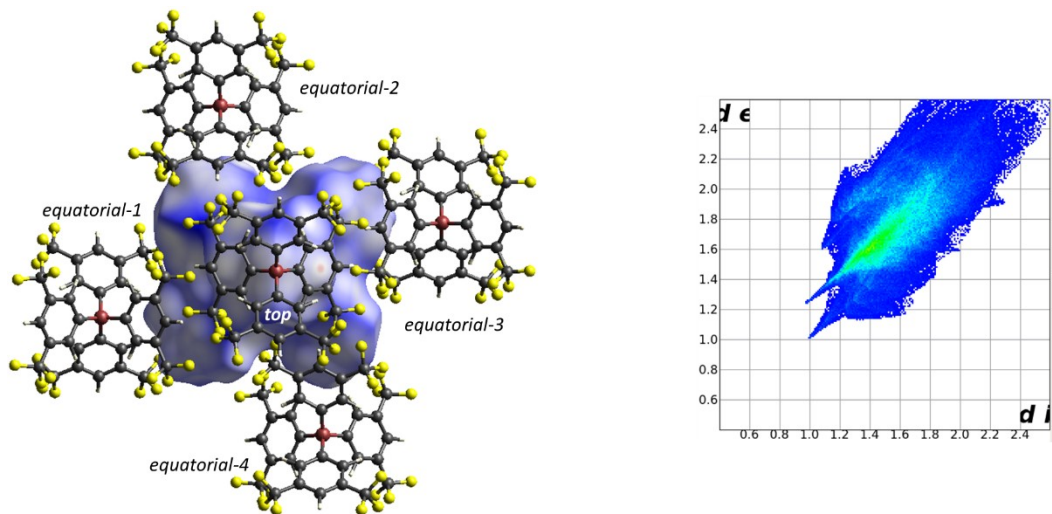
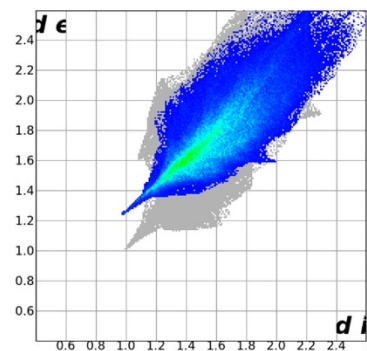
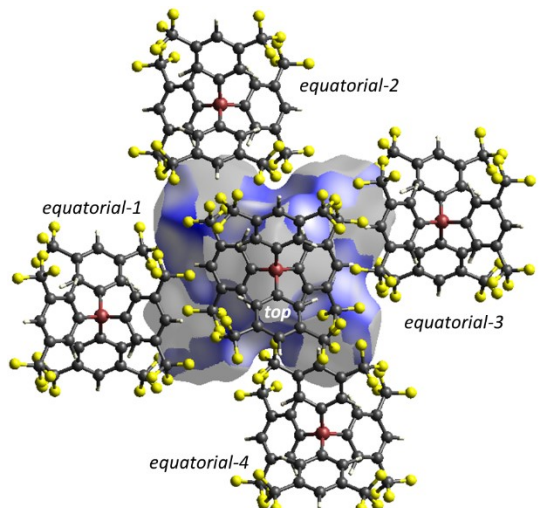
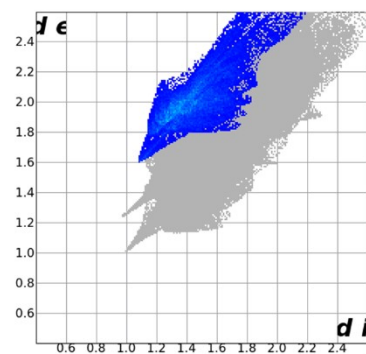
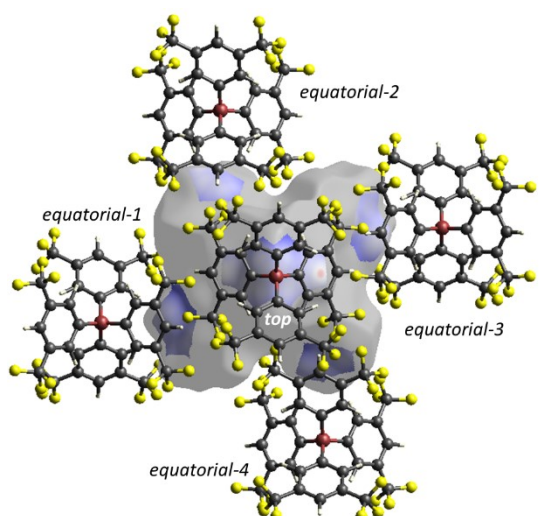


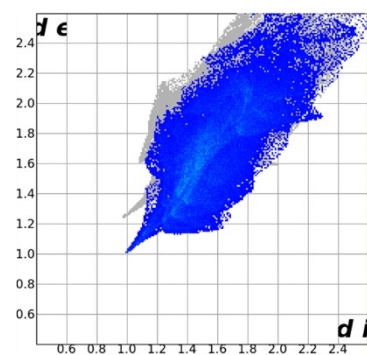
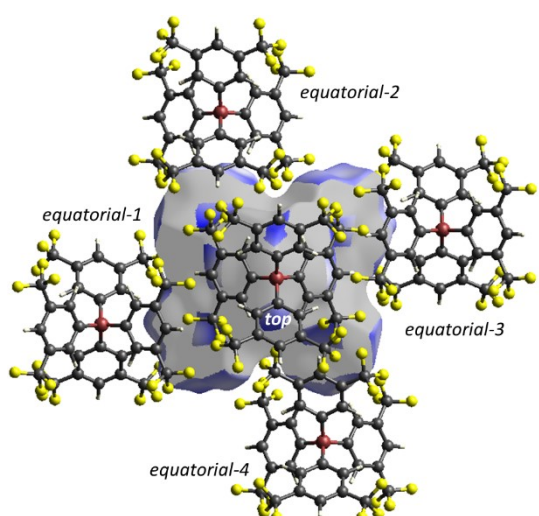
Figure S3. Hirshfeld surface mapped over d_{norm} for $[1\text{-NBA}]^+$ within the octahedral array of neighbouring $[\text{BArF}_4]^-$ anions. The accompanying fingerprint plot is also displayed. The view is taken from above the ‘top’ anion looking down the $\text{B}_{\text{top}} \square \text{Rh} \square \text{B}_{\text{bottom}}$ axis.



$$H_i \cdots F_e = 61.6\%$$



$$H_i \cdots C_e = 12.3\%$$



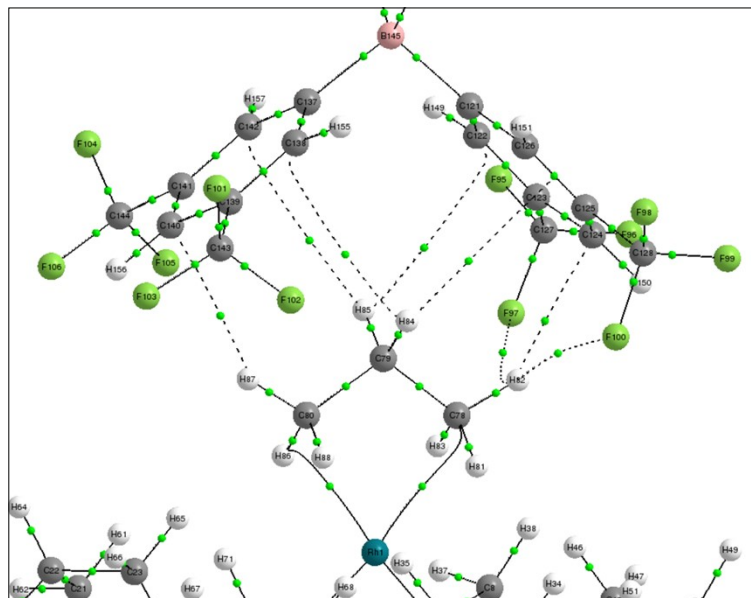
$$H_i \cdots H_e = 26.0\%$$

Figure S4. Hirshfeld surfaces for individual atom types mapped over d_{norm} for $[1\text{-NBA}]^+$ within the octahedral array of neighbouring $[\text{BArF}_4]^-$ anions. The accompanying fingerprint plot is also displayed. The views are taken from above the ‘top’ anion’ looking down the $\text{B}_{\text{top}} \square \text{Rh} \square \text{B}_{\text{bottom}}$ axis.

S3. QTAIM Analyses

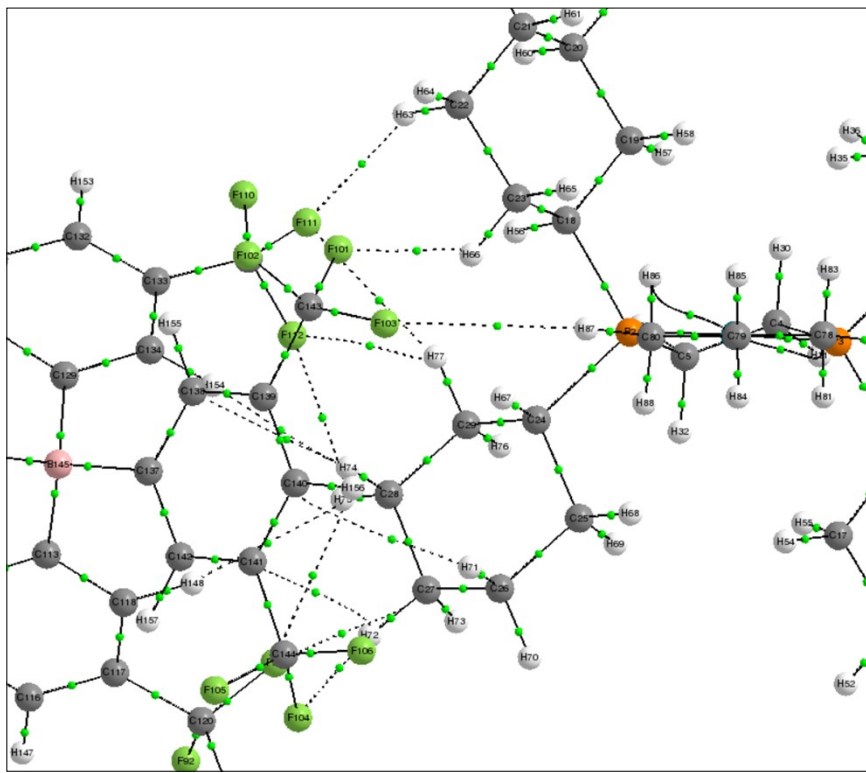
Molecular graphs for all ion pairs highlighting inter-ion bond paths are shown with bond critical bonds (BCPs) in green. Bond paths with $\rho(r) < 0.001$ a.u., intramolecular bond paths and ring critical points (RCP) are omitted for clarity. Tables of associated BCP metrics are also provided where all data are in atomic units ($\rho = e/\text{bohr}^3$; $\nabla^2\rho = e/\text{bohr}^5$; $H = \text{hartree}/\text{bohr}^3$, $q=e$). Atomic pair δG indices and % contribution computed via the IGMH approach are also presented. Separate atom labelling schemes are provided here, and these differ to those in the main manuscript.

S3.1 [1-propane][BAr^F₄]



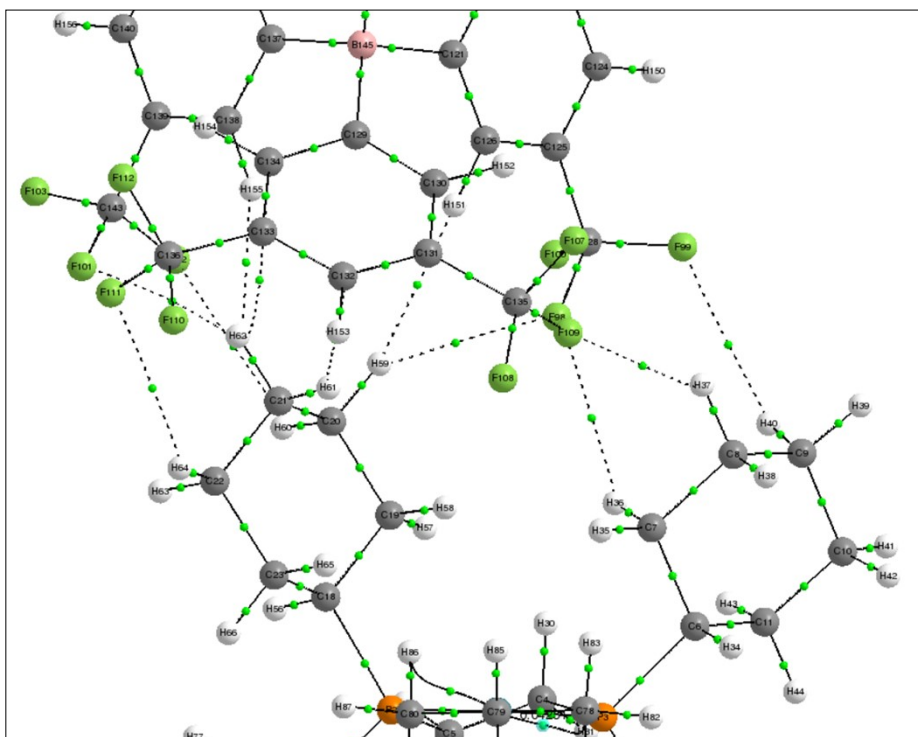
Bond Path	Distance/Å	$\rho(r)$	$\nabla^2\rho(r)$	H	DI	$\delta G_{\text{inter}} (\%)$
H82-F100	2.913	0.003247	+0.016127	0.001096	0.0076	0.012010 (1.19)
H82-F97	2.935	0.003306	+0.016538	0.001117	0.0069	0.012632 (1.25)
H87-C140	2.672	0.007804	+0.022744	0.001061	0.029975	0.026118 (2.59)
H84-C138	3.372	0.002391	+0.007473	0.000431	0.006101	0.008663 (0.86)
H85-C142	3.343	0.002406	+0.007545	0.000443	0.006624	0.010141 (1.01)
H85-C122	3.293	0.002755	+0.008578	0.000490	0.007462	0.009910 (0.98)
H84-C125	3.280	0.003063	+0.009447	0.000535	0.006843	0.010376 (1.03)
H82-C124	2.519	0.010279	+0.030680	0.001237	0.035605	0.036463 (3.62)

Figure S5. Molecular graph for the top ion-pair in [1-propane][BAr^F₄] along with associated BCP metrics for each bond path. Atomic pair δG indices and % contribution computed via the IGMH approach are also presented. All values are in atomic units.



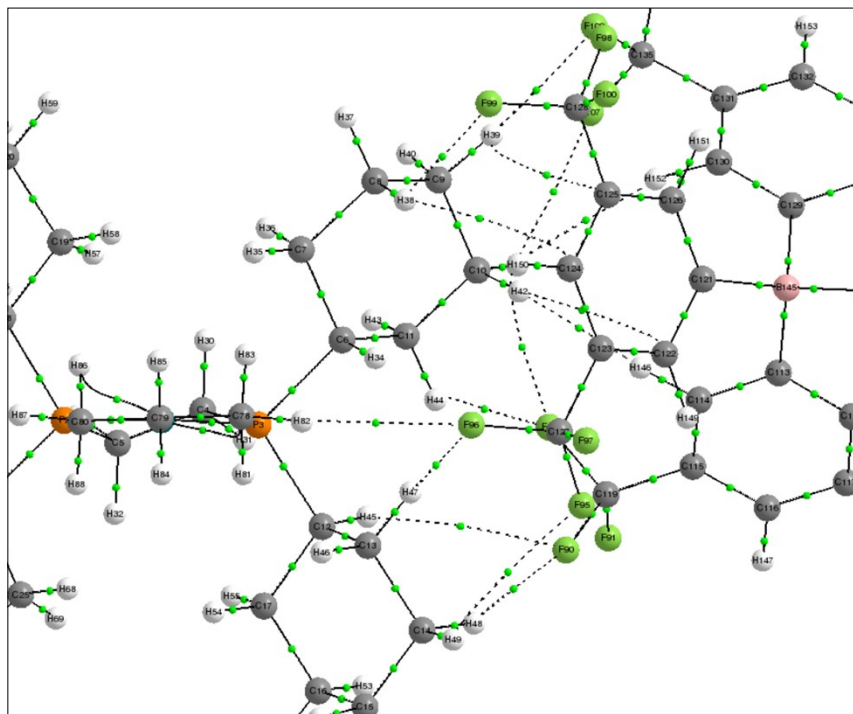
Bond Path	Distance/Å	$\rho(r)$	$\nabla^2\rho(r)$	H	DI	$\delta G_{\text{inter}} (\%)$
H63-F111	2.900	0.002399	+0.011871	0.000842	0.009270	0.007381 (0.64)
H66-F101	2.222	0.014120	+0.052426	0.000705	0.044357	0.046967 (4.10)
H87-F103	2.928	0.002181	+0.011103	0.000849	0.009962	0.006956 (0.61)
H72-F104	2.900	0.002810	+0.013862	0.000991	0.010458	0.009089 (0.79)
H75-F112	3.047	0.002044	+0.010892	0.000820	0.006397	0.006539 (0.57)
H75-F93	2.813	0.003418	+0.017190	0.001108	0.010584	0.013583 (1.19)
H77-F111	2.779	0.003836	+0.017116	0.001127	0.014277	0.014746 (1.29)
H77-F112	2.970	0.002687	+0.013404	0.001001	0.007611	0.009451 (0.83)
H71-C140	3.224	0.003022	+0.008589	0.000492	0.010317	0.011250 (0.98)
H74-C138	3.061	0.004244	+0.012904	0.000688	0.011331	0.017315 (1.51)
H72-C141	3.482	0.001987	+0.006642	0.000402	0.003464	0.008280 (0.72)
C27-F93	3.421	0.002859	+0.014749	0.000977	0.008724	0.009653 (0.84)
C28-H154	3.022	0.004430	+0.014443	0.000852	0.010699	0.015847 (1.38)
H75-H148	2.620	0.003458	+0.011666	0.000741	0.006941	0.012694 (1.11)

Figure S6. Molecular graph for the [1-propane][BAr^f₄] ion-pair formed with Eq-1 along with associated BCP metrics for each bond path. Atomic pair δG indices and % contribution computed via the IGMH approach are also presented. All values are in atomic units.



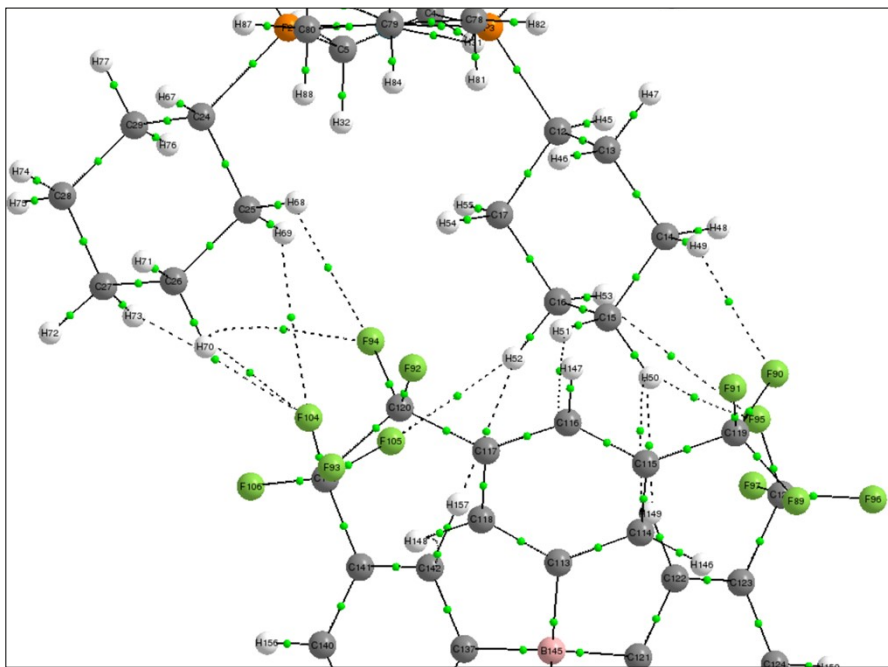
Bond Path	Distance/Å	$\rho(r)$	$\nabla^2\rho(r)$	H	DI	$\delta G_{\text{inter}} (\%)$
H40-F99	2.992	0.002222	+0.010911	0.000828	0.009563	0.006821 (0.82)
H37-F109	2.714	0.003953	+0.019039	0.001116	0.013598	0.015020 (1.81)
H36-F98	2.963	0.002242	+0.011275	0.000823	0.008498	0.006933 (0.84)
H59-F98	2.689	0.004513	+0.020608	0.001198	0.016707	0.017325 (2.09)
H60-F102	3.215	0.001270	+0.007056	0.000568	0.005065	0.005308 (0.64)
H64-F111	2.882	0.003032	+0.014825	0.001027	0.011999	0.008883 (1.07)
H62-F101	3.009	0.002193	+0.011039	0.000851	0.007805	0.007264 (0.88)
H61-C132	2.898	0.005584	+0.016750	0.000843	0.017844	0.022998 (2.78)
H62-C134	3.167	0.003632	+0.011209	0.000612	0.008968	0.015447 (1.86)
H62-H155	2.855	0.005579	+0.018409	0.001072	0.016225	0.022489 (2.71)
H59-H151	2.570	0.003182	+0.010186	-0.000695	0.009173	0.012447 (1.50)

Figure S7. Molecular graph for the [1-propane][BArF₄] ion-pair formed with Eq-2 along with associated BCP metrics for each bond path. Atomic pair δG indices and % contribution computed via the IGMH approach are also presented. All values are in atomic units.



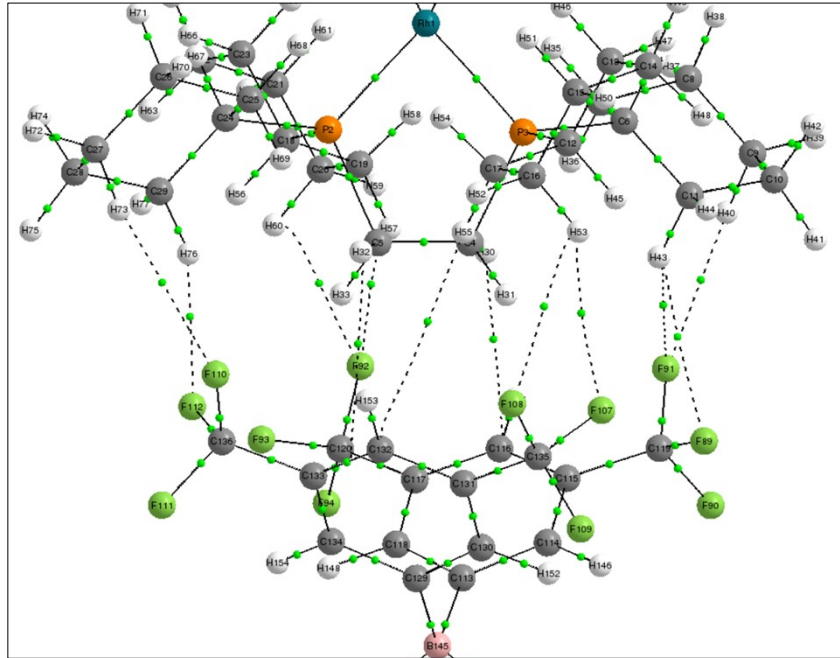
Bond Path	Distance/Å	$\rho(r)$	$\nabla^2\rho(r)$	H	DI	$\delta G_{\text{inter}} (\%)$
H47-F96	2.472	0.008163	+0.033054	0.001233	0.028353	0.028932 (2.42)
H45-F90	3.253	0.001204	+0.006359	0.000553	0.004381	0.006359 (0.53)
H48-F90	2.857	0.002704	+0.013018	0.000902	0.010607	0.008771 (0.73)
H49-F95	2.968	0.002649	+0.013464	0.000942	0.008559	0.007085 (0.59)
H82-F96	2.772	0.003289	+0.016394	0.001056	0.012591	0.012246 (1.02)
H44-F89	2.479	0.008144	+0.034149	0.001328	0.026240	0.026948 (2.25)
H41-F89	2.812	0.003948	+0.019741	0.001205	0.009964	0.015142 (1.27)
H41-F107	3.190	0.001328	+0.007306	0.000609	0.004874	0.006219 (0.52)
H38-F99	2.562	0.006654	+0.029007	0.001361	0.022047	0.025706 (2.15)
H39-F109	2.773	0.003791	+0.017922	0.001139	0.013968	0.013665 (1.14)
H42-C122	3.052	0.004362	+0.013081	0.000692	0.011646	0.017685 (1.48)
H38-C124	3.190	0.003187	+0.009478	0.000565	0.009595	0.012827 (1.07)
H39-C125	3.532	0.001875	+0.006346	0.000379	0.003662	0.006939 (0.58)
H42-H146	2.458	0.005009	+0.016566	0.000977	0.009807	0.022667 (1.89)
H41-H152	2.636	0.003427	+0.011603	0.000732	0.007280	0.012285 (1.03)

Figure S8. Molecular graph for the **[1-propane][BArF₄]** ion-pair formed with Eq-3 along with associated BCP metrics for each bond path. Atomic pair δG indices and % contribution computed via the IGMH approach are also presented. All values are in atomic units.



Bond Path	Distance/Å	$\rho(r)$	$\nabla^2\rho(r)$	H	DI	$\delta G_{\text{inter}} (\%)$
H68-F94	2.919	0.002397	+0.012271	0.000858	0.009033	0.008763 (0.83)
H69-F104	2.872	0.002948	+0.014767	0.000978	0.010242	0.011379 (1.08)
H70-F104	2.825	0.003309	+0.016846	0.001063	0.010102	0.012720 (1.20)
H70-F94	3.174	0.001532	+0.008483	0.000635	0.004852	0.004992 (0.47)
H73-F104	3.033	0.002194	+0.011623	0.000833	0.007514	0.007448 (0.70)
H52-F105	2.984	0.002353	+0.011266	0.000879	0.008944	0.008535 (0.81)
H50-F95	2.763	0.003966	+0.019418	0.001187	0.011494	0.017127 (1.62)
H53-F95	2.948	0.002577	+0.013439	0.000899	0.008289	0.008331 (0.79)
H49-F90	2.463	0.008158	+0.033421	0.001238	0.029155	0.026917 (2.55)
H51-C116	2.785	0.006959	+0.021356	0.001043	0.020671	0.028156 (2.66)
H50-C114	3.025	0.004610	+0.014343	0.000789	0.011734	0.020806 (1.97)
H52-H157	2.432	0.004209	+0.013683	0.000869	0.013221	0.020285 (1.92)
H50-H149	2.226	0.006427	+0.021340	0.001166	0.017287	0.029552 (2.79)

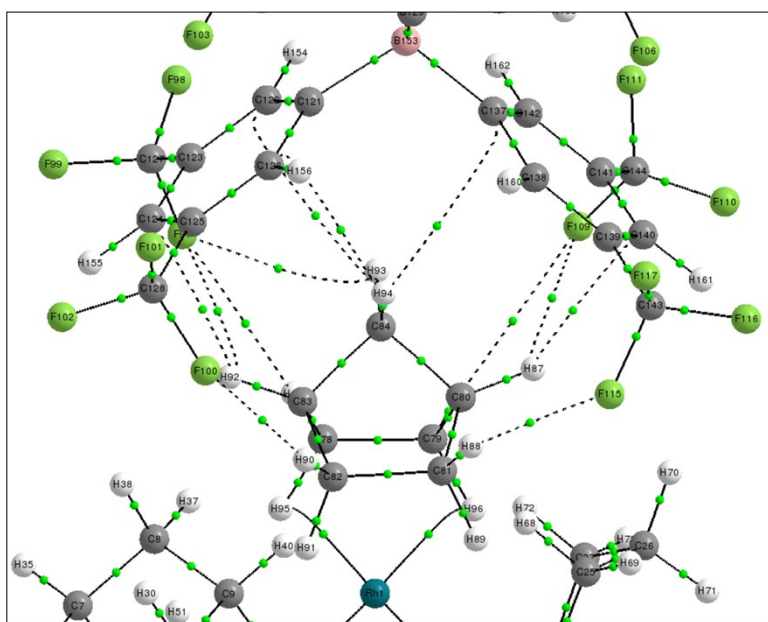
Figure S9. Molecular graph for the $[1\text{-propane}][\text{BArF}_4]$ ion-pair formed with Eq-4 along with associated BCP metrics for each bond path. Atomic pair δG indices and % contribution computed via the IGMH approach are also presented. All values are in atomic units.



Bond Path	Distance/Å	$\rho(r)$	$\nabla^2\rho(r)$	H	DI	$\delta G_{\text{inter}} (\%)$
H76-F112	2.344	0.010530	+0.038230	0.000779	0.036704	0.032934 (3.76)
H73-F110	2.894	0.002745	+0.013013	0.000933	0.011516	0.008786 (1.00)
H60-F92	2.505	0.008208	+0.036850	0.001605	0.022645	0.024038 (2.74)
H57-F92	2.711	0.004903	+0.023516	0.001340	0.014905	0.018652 (2.13)
H40-F91	2.544	0.006138	+0.026364	0.001182	0.021508	0.023406 (2.67)
H43-F91	2.578	0.004190	+0.019166	0.001196	0.013921	0.016375 (1.87)
H43-F89	2.892	0.003095	+0.014595	0.001058	0.010246	0.010545 (1.20)
H53-F108	2.843	0.003568	+0.017316	0.001135	0.011146	0.011974 (1.37)
H53-F107	2.995	0.002373	+0.011908	0.000929	0.008164	0.008462 (0.96)
H55-C132	3.543	0.001531	+0.004570	0.000297	0.005258	0.008311 (0.95)
H30-C116	3.623	0.001295	+0.004161	0.000279	0.004504	0.007240 (0.83)
H32-C132	3.637	0.001418	+0.004615	0.000303	0.003824	0.008089 (0.92)

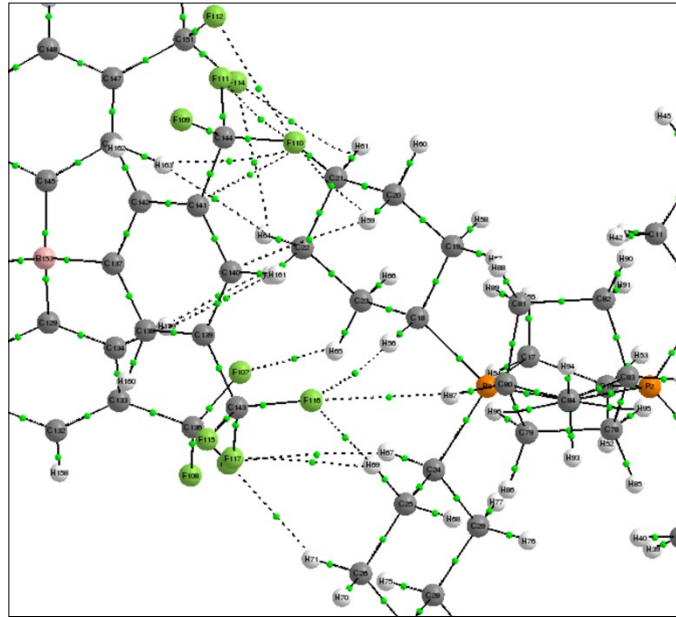
Figure S10. Molecular graph for the **[1-propane][BArF₄]** ion-pair formed with the bottom anion along with associated BCP metrics for each bond path. Atomic pair δG indices and % contribution computed via the IGMH approach are also presented. All values are in atomic units.

S3.2 [1-NBA][BAr^F₄]



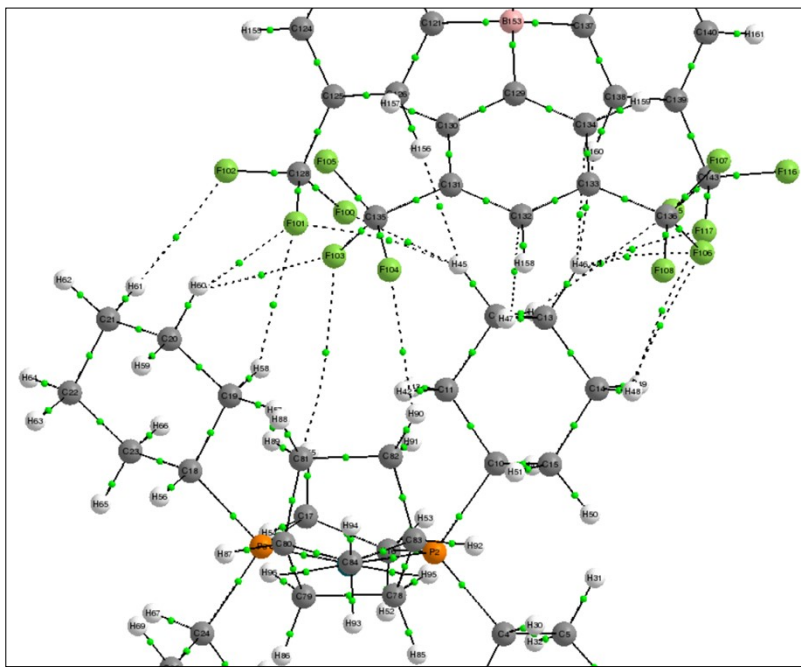
Bond Path	Distance/Å	$\rho(r)$	$\nabla^2\rho(r)$	H	DI	$\delta G_{\text{inter}} (\%)$
H90-F100	2.525	0.006658	+0.027204	0.001153	0.025332	0.023953 (1.72)
H92-F97	2.854	0.003768	+0.018654	0.001231	0.009930	0.015904 (1.14)
H85-F97	2.768	0.003599	+0.018141	0.001152	0.011961	0.014730 (1.06)
H93-F97	3.022	0.002598	+0.013489	0.000933	0.006588	0.009547 (0.68)
H86-F109	2.942	0.002376	+0.012531	0.000903	0.008365	0.007595 (0.54)
H87-F109	2.911	0.003286	+0.015772	0.001069	0.008816	0.012097 (0.87)
H88-F115	2.469	0.007718	+0.030890	0.001131	0.028373	0.025566 (1.83)
H92-C124	2.751	0.006863	+0.020971	0.001069	0.023658	0.024584 (1.76)
H93-C122	3.145	0.004254	+0.013405	0.000724	0.008693	0.017539 (1.26)
H94-C126	2.982	0.004870	+0.015094	0.000815	0.012894	0.019990 (1.43)
H94-C137	3.086	0.004072	+0.012707	0.000723	0.008806	0.017151 (1.23)
H87-H140	2.696	0.007704	+0.022973	0.001094	0.026801	0.026319 (1.89)

Figure S11. Molecular graph for the [1-NBA][BAr^F₄] ion-pair formed with the top anion along with associated BCP metrics for each bond path. Atomic pair δG indices and % contribution computed via the IGMH approach are also presented. All values are in atomic units.



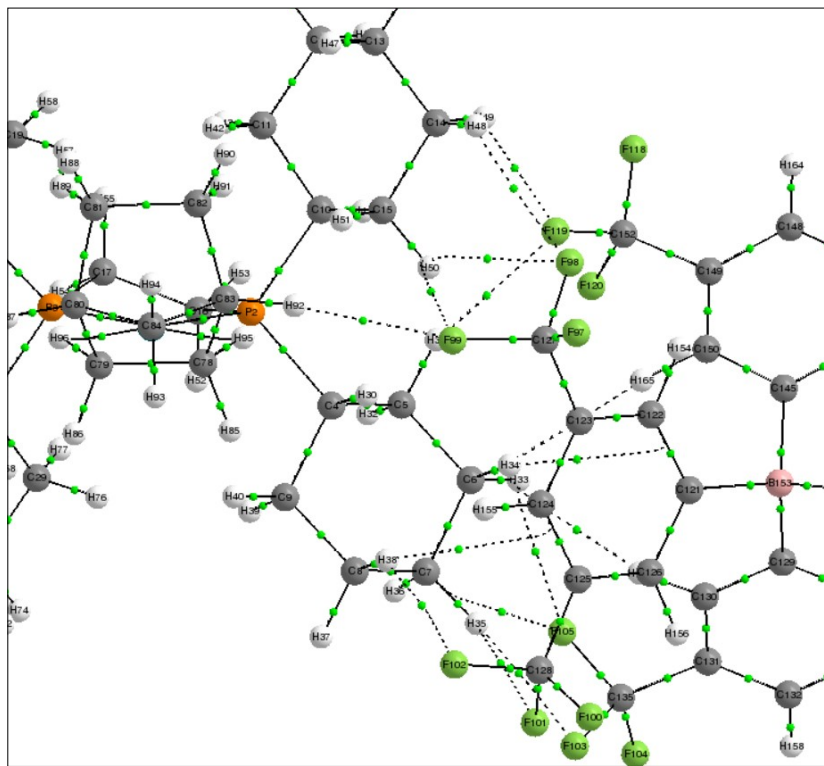
Bond Path	Distance/Å	$\rho(r)$	$\nabla^2\rho(r)$	H	DI	$\delta G_{\text{inter}} (\%)$
H71-F106	2.656	0.004557	+0.020417	0.001120	0.016766	0.018469 (1.33)
H67-F106	2.918	0.002796	+0.013176	0.000965	0.010047	0.010234 (0.74)
H69-F117	2.740	0.004276	+0.019682	0.001226	0.013995	0.015935 (1.15)
H69-F116	2.779	0.003957	+0.017792	0.001182	0.014288	0.015900 (1.14)
H87-F116	3.003	0.002005	+0.010251	0.000752	0.008156	0.005856 (0.42)
H56-F116	3.004	0.002290	+0.010628	0.000845	0.009108	0.009906 (0.71)
H65-F107	2.441	0.008775	+0.035549	0.001240	0.028233	0.029782 (2.14)
H59-F110	2.925	0.002928	+0.014465	0.001009	0.008891	0.010244 (0.74)
H64-F114	2.978	0.002503	+0.013205	0.000939	0.007280	0.008577 (0.62)
H61-F114	2.960	0.003157	+0.015818	0.001051	0.007809	0.009761 (0.70)
H62-F112	2.858	0.003271	+0.015622	0.001075	0.011245	0.011225 (0.81)
H62-F111	2.976	0.002413	+0.011602	0.000880	0.008556	0.008858 (0.64)
H63-C138	2.940	0.005401	+0.016337	0.000834	0.014129	0.022703 (1.63)
H59-C140	3.003	0.004291	+0.012416	0.000686	0.014756	0.020082 (1.44)
H62-C141	3.306	0.002668	+0.008534	0.000500	0.005737	0.010321 (0.74)
H64-H163	2.448	0.004953	+0.017547	0.001091	0.010592	0.018762 (1.35)
H63-H159	2.399	0.005762	+0.019563	0.001132	0.010701	0.021559 (1.55)
H62-H163	2.539	0.003869	+0.013320	0.000810	0.007824	0.015749 (1.13)

Figure S12. Molecular graph for the **[1-NBA][BArF₄]** ion-pair formed with Eq-1 along with associated BCP metrics for each bond path. Atomic pair δG indices and % contribution computed via the IGMH approach are also presented. All values are in atomic units.



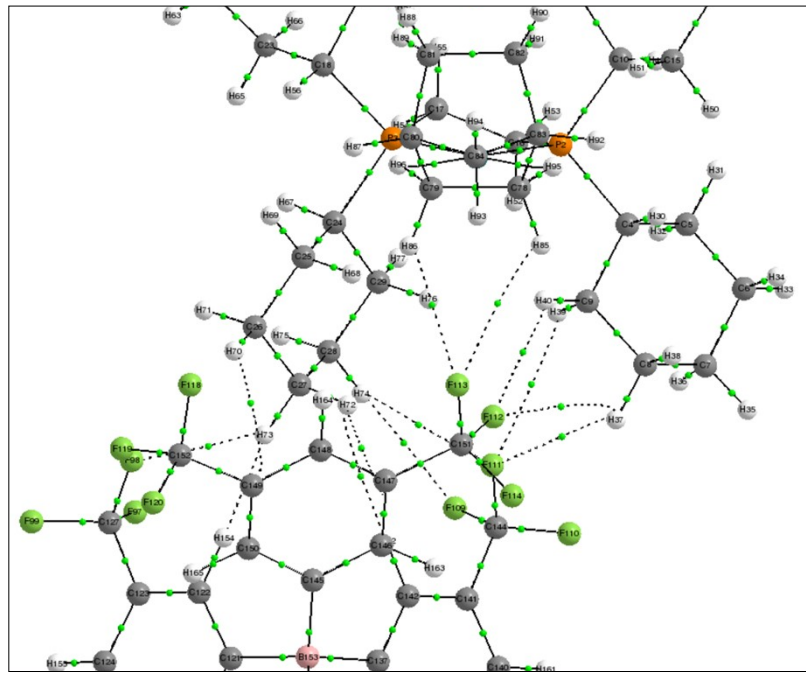
Bond Path	Distance/Å	$\rho(r)$	$\nabla^2\rho(r)$	H	DI	$\delta G_{\text{inter}} (\%)$
H61-F102	2.705	0.004586	+0.019990	0.001173	0.017724	0.016732 (1.35)
H60-F101	2.558	0.006664	+0.030807	0.001480	0.019218	0.021980 (1.77)
H60-F103	3.142	0.001326	+0.007261	0.000568	0.004969	0.005031 (0.40)
H58-F101	2.557	0.006847	+0.030615	0.001426	0.021601	0.024481 (1.97)
H90-F104	2.599	0.005817	+0.025684	0.001301	0.021247	0.022297 (1.79)
H81-F103	3.585	0.001811	+0.009872	0.000728	0.005692	0.005172 (0.42)
H45-F101	2.890	0.003229	+0.015405	0.001077	0.008216	0.012519 (1.01)
H45-F100	2.804	0.003893	+0.017888	0.001175	0.012611	0.014378 (1.16)
H44-F115	3.267	0.001188	+0.006248	0.000540	0.004711	0.005645 (0.45)
H49-F117	2.933	0.002648	+0.013777	0.000917	0.008450	0.008693 (0.70)
H48-F106	2.946	0.002598	+0.013148	0.000933	0.009869	0.007445 (0.60)
H46-F117	2.726	0.004504	+0.021649	0.001284	0.012597	0.019367 (1.56)
H46-F106	2.965	0.002761	+0.013517	0.000965	0.007104	0.009762 (0.78)
H47-C132	3.093	0.004017	+0.012007	0.000634	0.012692	0.016003 (1.29)
H46-C134	3.005	0.004660	+0.014256	0.000786	0.011875	0.020832 (1.67)
H45-H156	2.220	0.006595	+0.021939	0.001202	0.019227	0.022413 (1.80)
H46-H160	3.067	0.007880	+0.025994	0.001233	0.020232	0.028216 (2.27)

Figure S13. Molecular graph for the $[1\text{-NBA}][\text{BAr}_4]$ ion-pair formed with Eq-2 along with associated BCP metrics for each bond path. Atomic pair δG indices and % contribution computed via the IGMH approach are also presented. All values are in atomic units.



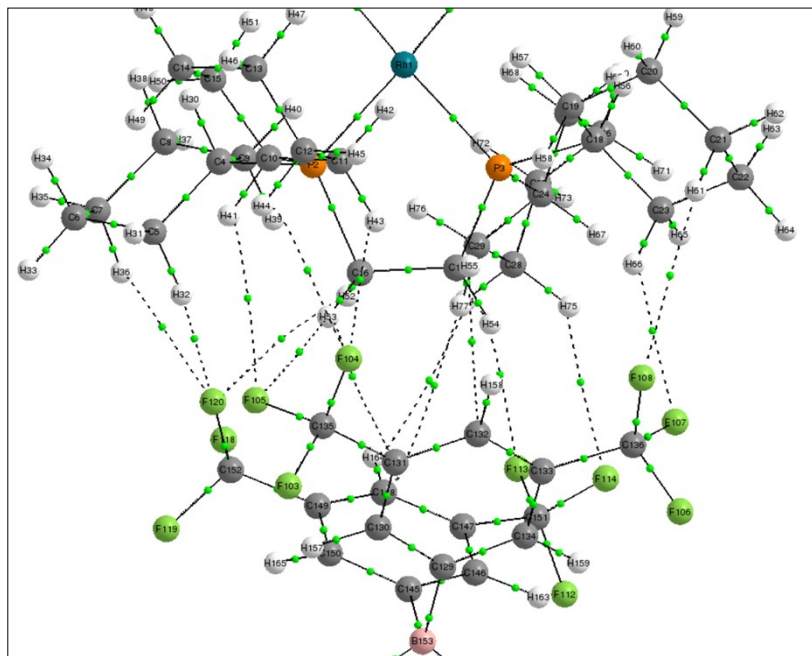
Bond Path	Distance/Å	$\rho(r)$	$\nabla^2\rho(r)$	H	DI	$\delta G_{\text{inter}} (\%)$
H49-F119	2.670	0.004757	+0.021515	0.001171	0.017474	0.019595 (1.30)
H48-F98	2.587	0.006088	+0.027296	0.001339	0.020504	0.022917 (1.52)
H50-F98	2.816	0.004051	+0.019721	0.001265	0.010645	0.015543 (1.03)
H50-F99	2.841	0.004169	+0.020059	0.001284	0.009761	0.016480 (1.09)
H92-F99	2.813	0.003244	+0.015676	0.001021	0.012895	0.011342 (0.75)
H31-F119	2.403	0.009124	+0.034556	0.000963	0.031446	0.032079 (2.13)
H33-F105	2.743	0.004299	+0.021069	0.001267	0.012833	0.018000 (1.19)
H38-F102	2.875	0.003287	+0.015354	0.001053	0.010958	0.011552 (0.77)
H35-F103	2.649	0.005370	+0.023676	0.001289	0.018243	0.020677 (1.37)
H35-F101	2.961	0.002406	+0.012191	0.000899	0.008319	0.008030 (0.53)
H34-C122	3.069	0.004371	+0.013049	0.000704	0.011119	0.016841 (1.12)
H38-C124	3.141	0.003688	+0.010520	0.000593	0.011139	0.015046 (1.00)
C7-F105	3.261	0.004296	+0.021112	0.001306	0.012258	0.019032 (1.26)
H34-H165	2.435	0.005183	+0.017286	0.001016	0.010325	0.022706 (1.50)
H33-H157	2.427	0.005441	+0.019608	0.001189	0.010142	0.022844 (1.51)

Figure S14. Molecular graph for the $[1\text{-NBA}][\text{BArF}_4]$ ion-pair formed with Eq-3 along with associated BCP metrics for each bond path. Atomic pair δG indices and % contribution computed via the IGMH approach are also presented. All values are in atomic units.



Bond Path	Distance/Å	$\rho(r)$	$\nabla^2\rho(r)$	H	DI	$\delta G_{\text{inter}} (\%)$
H37-F111	2.791	0.003712	+0.018029	0.001145	0.013217	0.013786 (1.25)
H37-F112	2.927	0.002793	+0.014281	0.000925	0.007593	0.009600 (0.87)
H39-F111	2.946	0.002628	+0.013510	0.000916	0.008360	0.008593 (0.78)
H40-F112	2.684	0.004409	+0.021067	0.001215	0.016043	0.021391 (1.93)
H85-F113	2.913	0.002748	+0.013916	0.000983	0.010268	0.010082 (0.91)
H86-F113	2.647	0.004875	+0.022559	0.001273	0.018365	0.020162 (1.82)
H74-F111	2.779	0.004070	+0.019547	0.001232	0.012267	0.015703 (1.42)
H74-F109	2.812	0.003587	+0.016109	0.001115	0.013466	0.013119 (1.19)
H73-F98	2.476	0.007899	+0.033132	0.001278	0.024401	0.028124 (2.54)
H72-C147	3.231	0.003108	+0.009305	0.000528	0.008856	0.011452 (1.04)
H70-C149	3.140	0.003441	+0.010225	0.000591	0.010442	0.011426 (1.03)
H72-H162	2.560	0.003783	+0.012268	0.000761	0.008232	0.017232 (1.56)
H73-H154	2.001	0.010167	+0.031975	0.001145	0.027311	0.033050 (2.99)

Figure S15. Molecular graph for the [1-NBA][BAr^F₄] ion-pair formed with Eq-4 along with associated BCP metrics for each bond path. Atomic pair δG indices and % contribution computed via the IGMH approach are also presented. All values are in atomic units.



Bond Path	Distance/Å	$\rho(r)$	$\nabla^2\rho(r)$	H	DI	$\delta G_{\text{inter}} (\%)$
H41-F105	3.057	0.001929	+0.009772	0.000763	0.007220	0.007010 (0.61)
H44-F104	2.760	0.004468	+0.021507	0.001273	0.013393	0.016559 (1.44)
H43-F104	2.699	0.004984	+0.022981	0.001309	0.016482	0.020223 (1.76)
H36-F120	2.747	0.004334	+0.019961	0.001208	0.015415	0.017101 (1.48)
H32-F120	2.202	0.012974	+0.048697	0.000662	0.041269	0.047183 (4.10)
H74-F113	2.812	0.004060	+0.019868	0.001258	0.011624	0.014944 (1.30)
H75-F114	2.792	0.003841	+0.017678	0.001146	0.014244	0.012947 (1.12)
H77-C148	3.423	0.002032	+0.006036	0.000367	0.007214	0.007589 (0.66)
H74-H164	2.865	0.002118	+0.006874	0.000466	0.004738	0.010393 (0.90)
H66-F107	2.565	0.006720	+0.028727	0.001353	0.022090	0.025210 (2.19)
H61-F108	3.053	0.001821	+0.009433	0.000721	0.006779	0.005944 (0.52)
H52-F120	2.965	0.002421	+0.011980	0.000901	0.008030	0.009484 (0.82)
H53-F105	2.756	0.003883	+0.017492	0.001162	0.015168	0.014382 (1.25)
H55-C132	3.136	0.003496	+0.010383	0.000591	0.011611	0.014121 (1.23)
H53-C131	3.293	0.002458	+0.008075	0.000538	0.006651	0.009934 (0.86)

Figure S16. Molecular graph for the **[1-NBA][BArF₄]** ion-pair formed with the bottom anion along with associated BCP metrics for each bond path. Atomic pair δG indices and % contribution computed via the IGMH approach are also presented. All values are in atomic units.

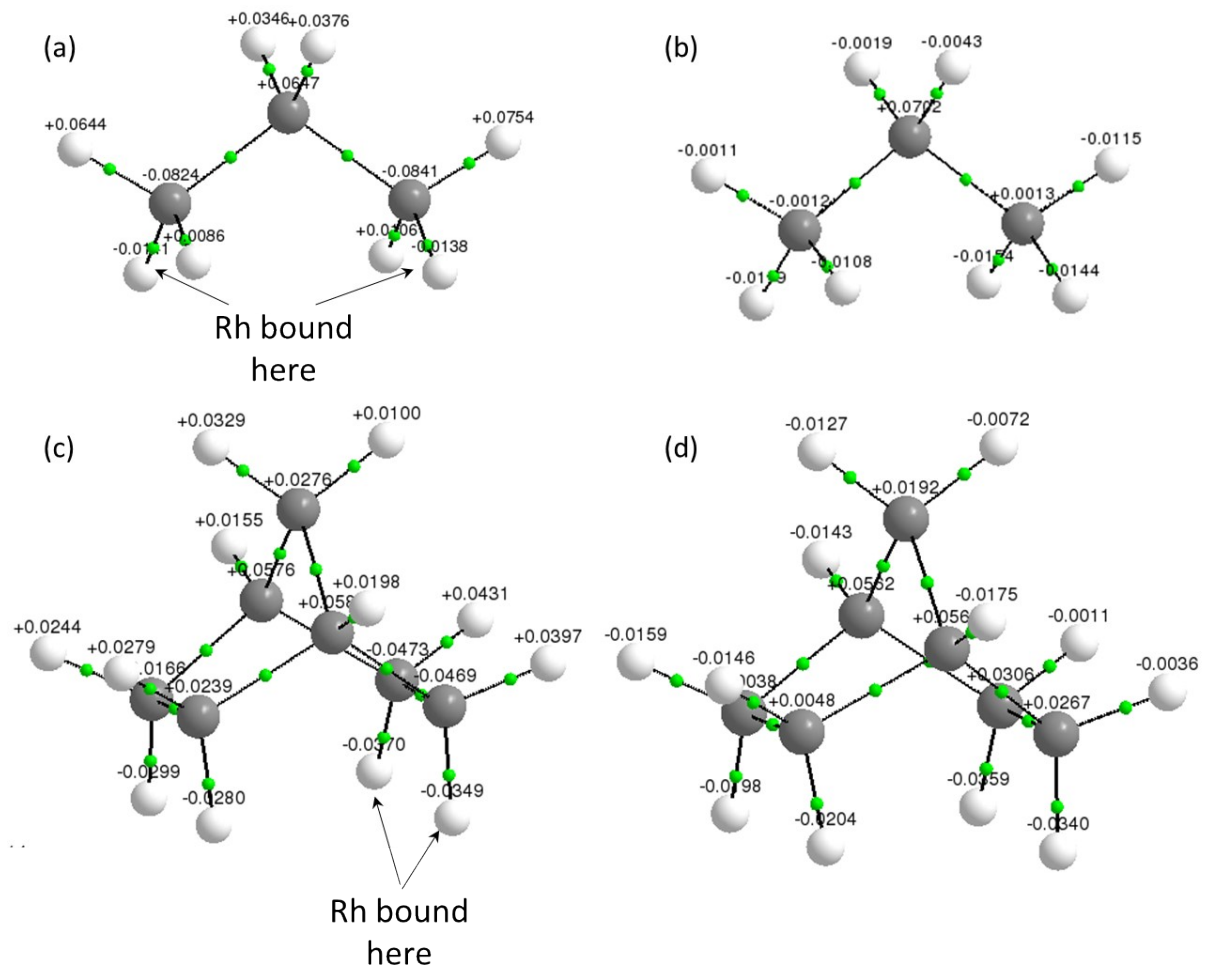


Figure S17. Computed QTAIM charges on the propane and NBA ligands computed with [(a)/(c)] and without [(b)/(d)] the $\{\text{Cy}_2\text{PCH}_2\text{CH}_2\text{PCy}_2\}\text{Rh}$ fragment. $\{\text{Cy}_2\text{PCH}_2\text{CH}_2\text{PCy}_2\}\text{Rh}$ and top $[\text{BAr}^{\text{F}}_4]^-$ anion not shown.

S4. IGMH Plots

S4.1. [1-propane][BAr^F₄]

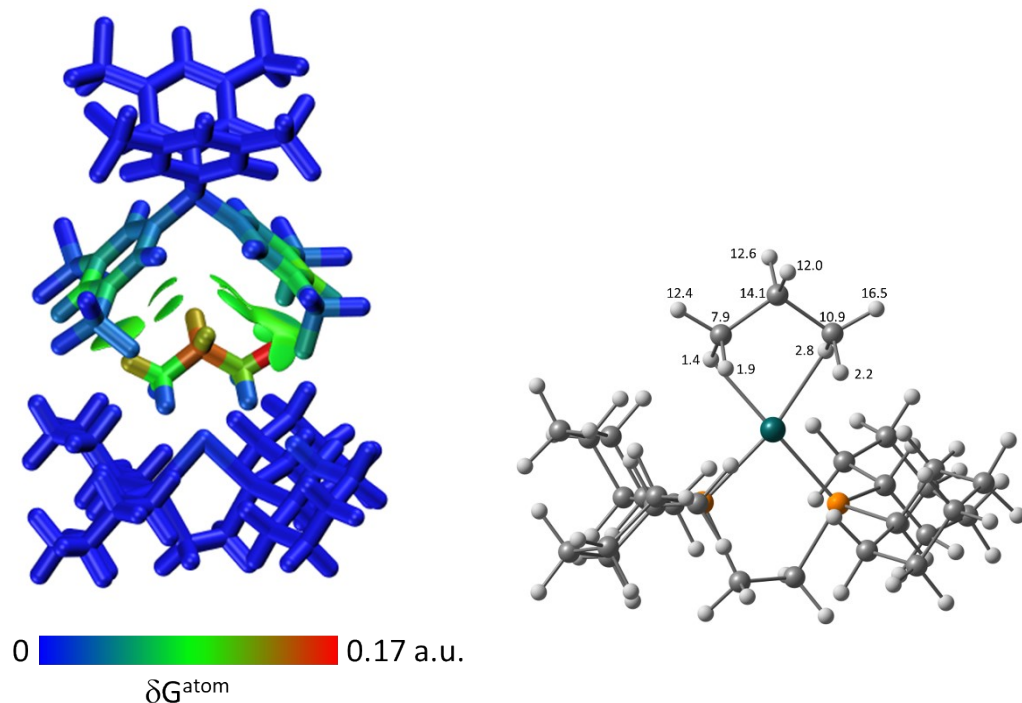


Figure S18. IGMH plots for the [1-propane][BAr^F₄] ion-pair formed with the top anion with the cation and anion are defined as separate fragments and sign(λ_2) ρ -coloured isosurfaces are plotted with $\delta g^{\text{inter}} = 0.003$ a.u. Atomic % contributions are coloured by δG^{atom} and absolute values above 1% from the cation are indicated in the ball and stick model.

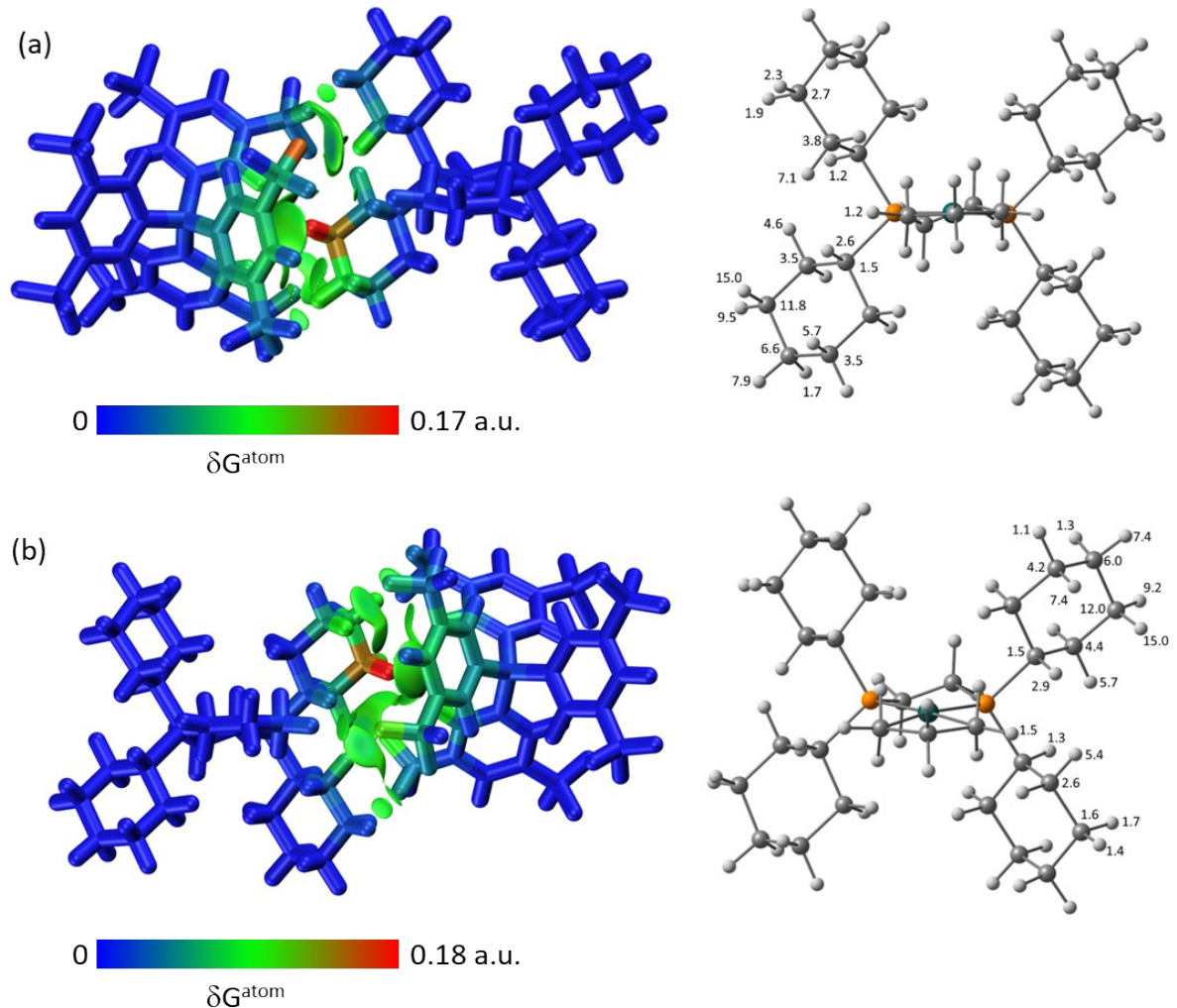


Figure S19. IGMH plots for the **[1-propane][BAr^F₄]** ion-pairs formed with (a) the Eq-1 anion and (b) the Eq-3 anion, with the cation and anions defined as separate fragments and sign(λ_2) ρ -coloured isosurfaces are plotted with $\delta g^{\text{inter}} = 0.003$ a.u. Atomic % contributions are coloured by δG^{atom} and absolute values above 1% from the cation are indicated in the ball and stick models.

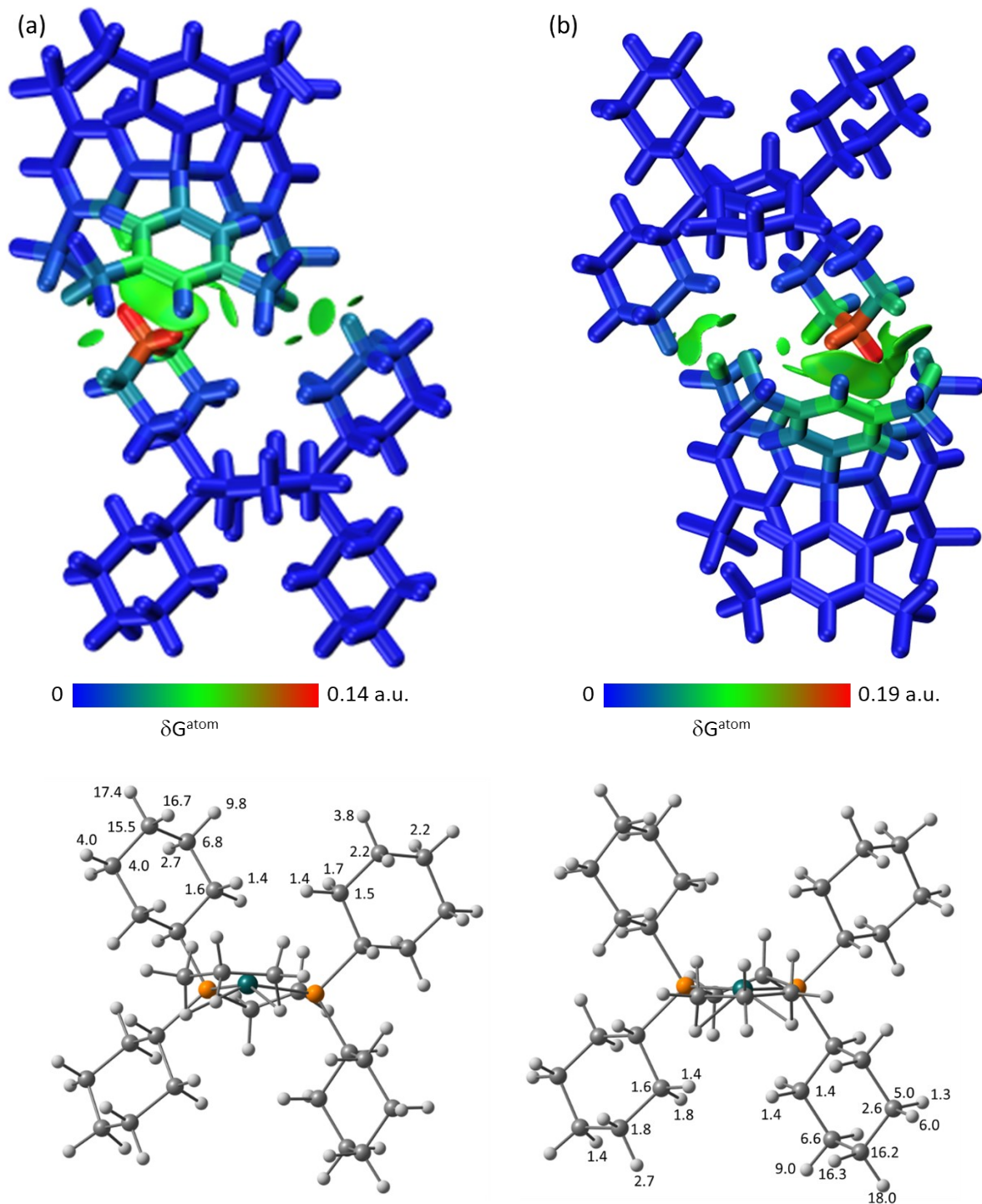


Figure S20. IGMH plots for the **[1-propane][BArF₄]** ion-pairs formed with (a) the Eq-2 anion and (b) the Eq-4 anion, with the cation and anions defined as separate fragments and sign(λ_2) ρ -coloured isosurfaces are plotted with $\delta g^{\text{inter}} = 0.003$ a.u. Atomic % contributions are coloured by $\delta G_{\text{atom}}^{\text{inter}}$ and absolute values above 1% from the cation are indicated in the ball and stick models.

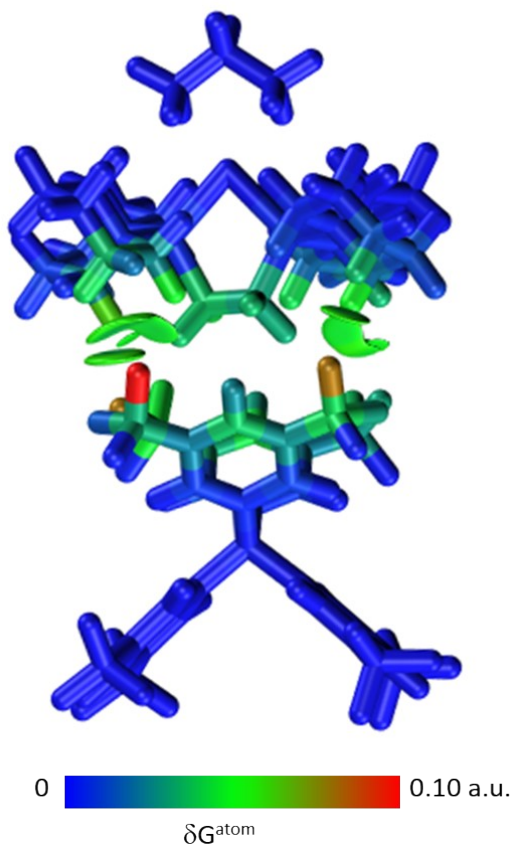


Figure S21. IGMH plot for the [1-propane][BArF₄] ion-pair formed with the bottom anion with the cation and anion are defined as separate fragments and sign(λ_2) ρ -coloured isosurfaces are plotted with $\delta g^{\text{inter}} = 0.003$ a.u. Atomic % contributions are coloured by $\delta G_{\text{atom}}^{\text{atom}}$.

S4.2. [1-NBA][BAr^F₄]

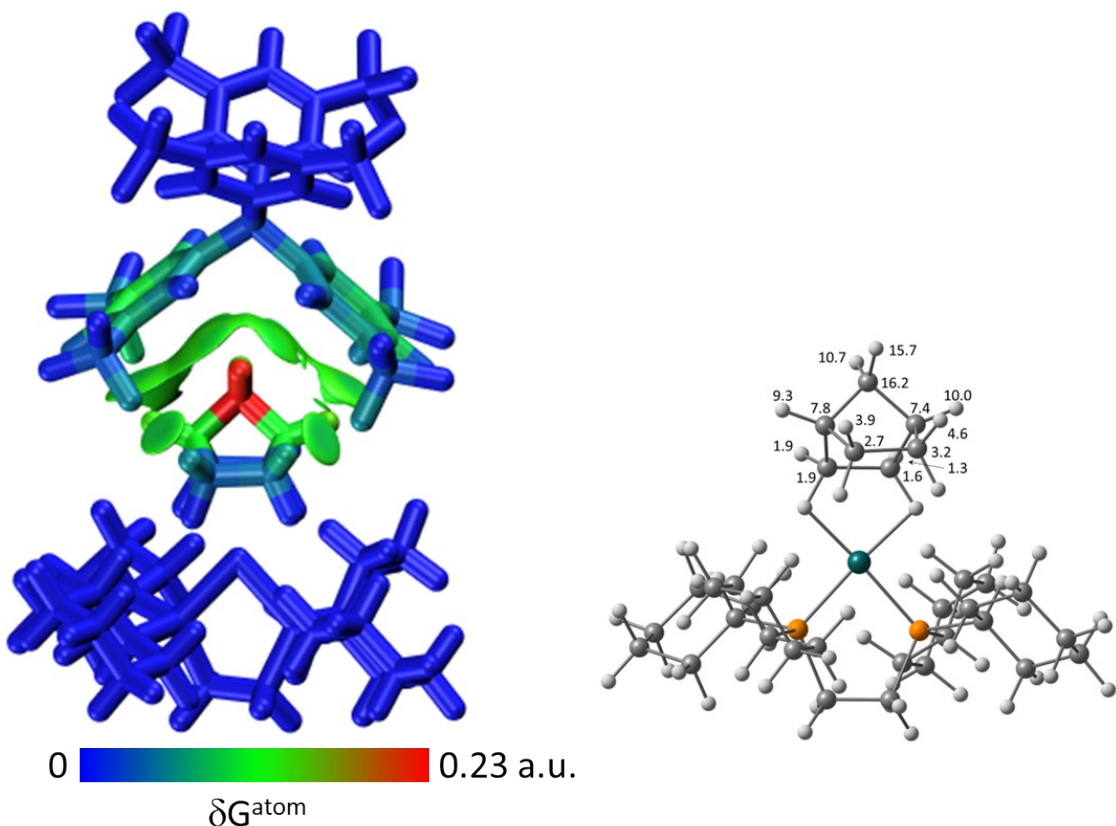


Figure S22. IGMH plots for the [1-NBA][BAr^F₄] ion-pair formed with the top anion with the cation and anion are defined as separate fragments and sign(λ_2) ρ -coloured isosurfaces are plotted with $\delta g^{\text{inter}} = 0.003$ a.u. Atomic % contributions are coloured by δG^{atom} and absolute values above 1% from the cation are indicated in the ball and stick model.

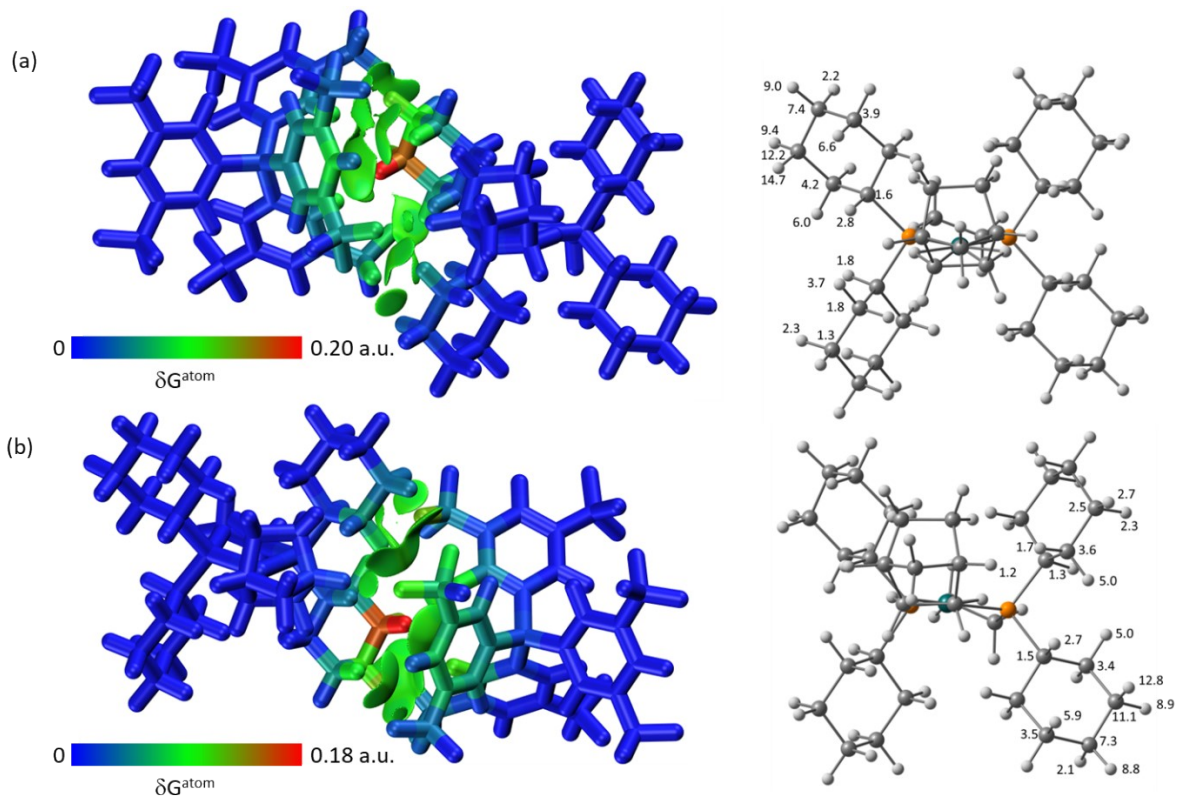


Figure S23. IGMH plots for the $[1\text{-NBA}][\text{BArF}_4]$ ion-pairs formed with (a) the Eq-1 anion and (b) the Eq-3 anion, with the cation and anions defined as separate fragments and $\text{sign}(\lambda_2)\rho$ -coloured isosurfaces are plotted with $\delta g^{\text{inter}} = 0.003 \text{ a.u.}$ Atomic % contributions are coloured by δG^{atom} and absolute values above 1% from the cation are indicated in the ball and stick models.

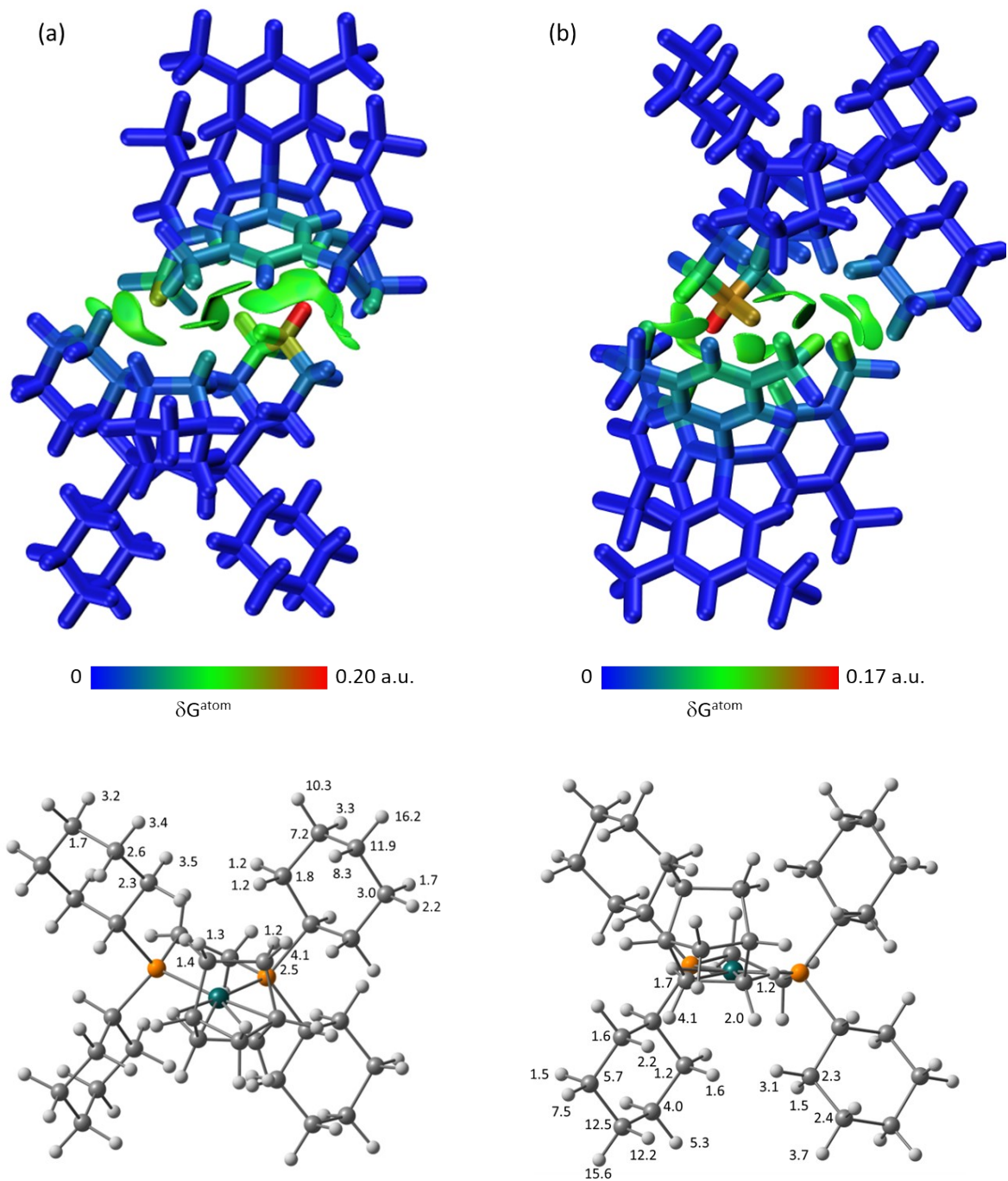


Figure S24. IGMH plots for the $[1\text{-NBA}][\text{BArF}_4]$ ion-pairs formed with (a) the Eq-2 anion and (b) the Eq-4 anion, with the cation and anions defined as separate fragments and $\text{sign}(\lambda_2)\rho$ -coloured isosurfaces are plotted with $\delta g^{\text{inter}} = 0.003$ a.u. Atomic % contributions are coloured by δG_{atom} and absolute values above 1% from the cation are indicated in the ball and stick models.

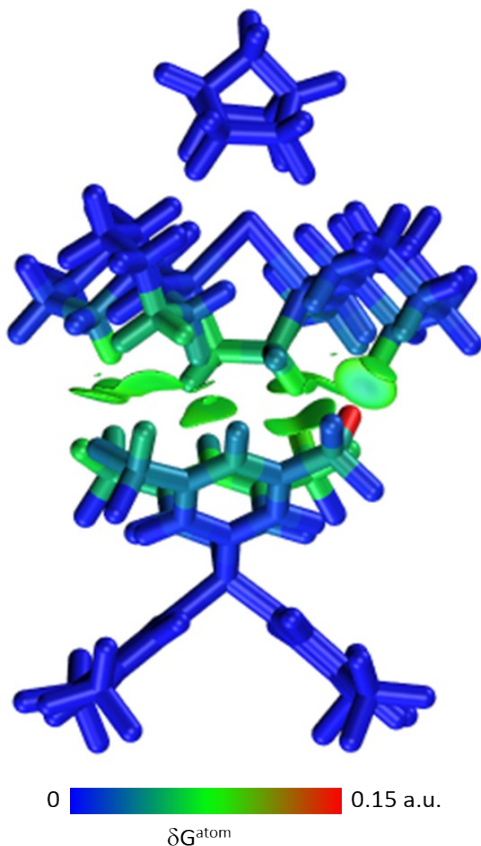


Figure S25. IGMH plot for the [1-propane][BAr^f₄] ion-pair formed with the bottom anion with the cation and anion are defined as separate fragments and sign(λ_2) ρ -coloured isosurfaces are plotted with $\delta g^{\text{inter}} = 0.003$ a.u. Atomic % contributions are coloured by δG^{atom} .

S5. Correlation Plots.

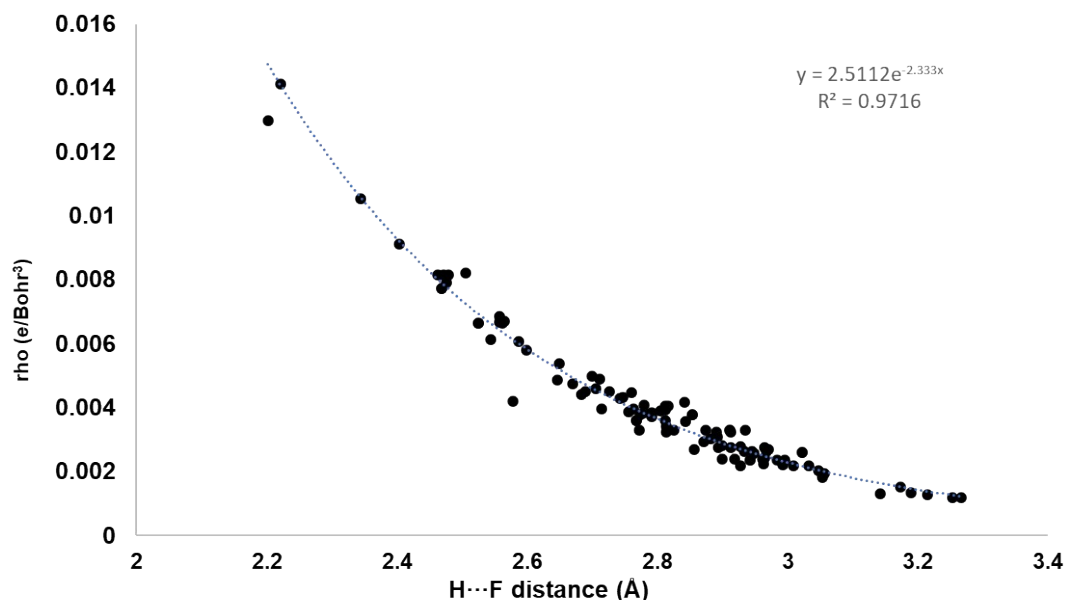


Figure S26. Plot of $\rho(r)$ vs H···F distance for all C–H···F bond paths in [1-propane][BAr^F₄] and [1-NBA][BAr^F₄].

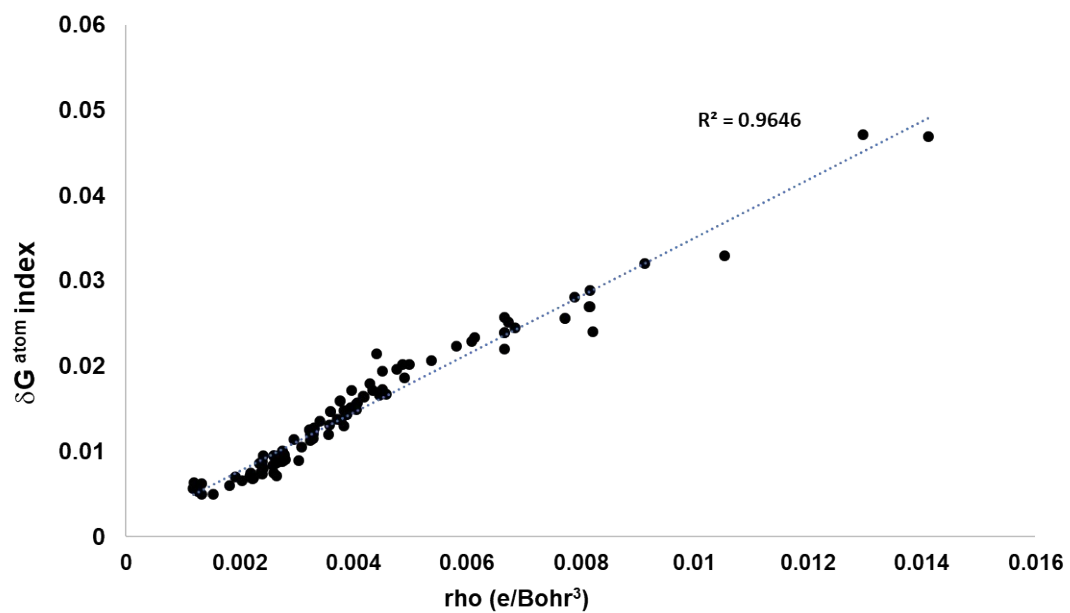


Figure S27. Plot of $\rho(r)$ vs δG_{atom} index for all C–H···F bond paths in [1-propane][BAr^F₄] and [1-NBA][BAr^F₄].